

Study on sintering process of woodceramics from the cashew nutshell waste

Kieu Do Trung Kien^a, Phan Dinh Tuan^b, Toshihiro Okabe^c, Do Quang Minh^a and Tran Van Khai^{a,*}

^aFaculty of Materials Technology, Ho Chi Minh city University of Technology, VNU-HCM, 268 Ly Thuong Kiet street, Ward 14, District 10, Ho Chi Minh City, Viet Nam

^bResearch Institute for Sustainable Development, Hochiminh City University of Natural Resources and Environment, 236B Le Van Sy Street, Ward 1, Tan Binh District, Ho Chi Minh, Viet Nam

^cShibaura Institute of Technology Graduate school Cooperative Graduate School System, 3-7-5 Toyosu, Koto-ku, Tokyo 135-8548, Japan

In this study, the sintering mechanism of woodceramics (WCs) from cashew nut shell waste (CNSW) was studied by analyzing chemical reactions and structural changes during the sintering process of CNSW powder, liquefied wood and green bodies of WCs at 900 °C for 60 minutes in the CO₂ atmosphere. The chemical and structural properties of the products were investigated by X-ray diffraction (XRD), Raman spectroscopy, Fourier Transform Infrared (FTIR), and scanning electron microscope (SEM). The results showed that the decomposition reactions of liquefied wood and CNSW occurred simultaneously to form the hard carbon and the soft carbon at high temperature. The sintering mechanism of WCs has been presented.

Key words: Woodceramics, Liquefied wood, Cashew nut shell waste, Hard carbon, Soft carbon.

Introduction

Carbon that is crystalline base material like diamonds, graphite or carbon nanotubes (CNT) has many practical applications thanks to their special properties. Therefore, the carbon crystalline materials are being used in various scientific and technical fields such as activated carbon [1], electrodes [2], refractories [3], semiconductors [4], superconductors [5], drug distribution [6].

Amorphous carbon materials also have important applications. WCs are a kind of amorphous carbon materials that being sintered at high temperature in non-oxygenated atmosphere. WCs, which was first developed in 1995 [7], were initially based on various types of wood materials being fabricated after the ceramic process finished. At microstructure scale, WCs were composite materials of soft carbon and hard carbon [8]. Soft carbon was the thermal decomposition product of wood pulp and hard carbon was the thermal decomposition product of liquefied wood [9]. Depending on their graphitizability, the amorphous carbon materials are usually divided into two types, hard carbon (Fig. 1(a)) and soft carbon (Fig. 1(b)). Soft carbon can be transformed into graphite after heat treatment at 2800 °C or higher, while hard carbon cannot be transformed.

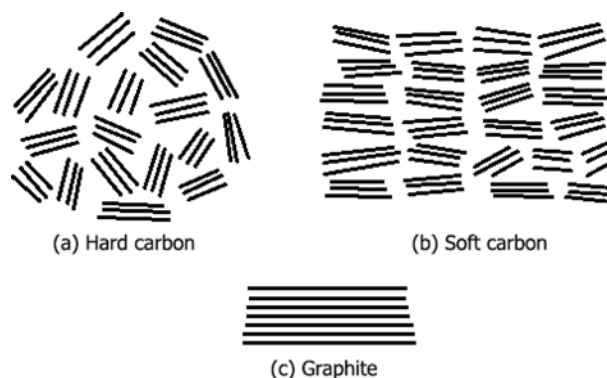


Fig. 1. The structural models of hard carbon (a), soft carbon (b) and graphite (c).

WCs also have the good properties such as high mechanical strength, high abrasion resistance, high porosity, biological inertia, electromagnetic shielding, corrosion resistance, therefore WCs have been applied to the type materials such as a sensor, electrode polymer, electrolyte fuel cell, absorber of an electromagnetic wave, heat source [10]. WCs have been fabricated from biomass materials such as bagasse [11], wood pulp [12], bamboo [13]. The general technique was to mix biomass materials with liquefied wood and heated the samples at 600-1500 °C.

In this study, the WC samples from CNSW were mixed with the liquefied and being sintered altogether at 900 °C in CO₂ atmosphere. The phase composition, chemical and morphological changes of the as-prepared samples were analyzed by XRD, Raman, FTIR spectroscopy and SEM.

*Corresponding author:
Tel : +84.8-8-661 320
Fax: +84.8-8-661 843
E-mail: tvkhai1509@gmail.com

Experimental

The raw material of CNSW was taken from Binh Phuoc province, South East of Vietnam. Its chemical compositions are shown in Table 1. It was cleaned by water then crushed into powder and then filtered through the sieve of 500 μm to bring sample to particle size (Fig. 2(a)). The liquefied wood (Fig. 2(b)) was prepared by heating the 3-component mixtures of CNSW powder, phenol solution (96%) and sulfuric acid solution (98%) at 140 $^{\circ}\text{C}$ for 4 hrs. The green body of WCs, dimension of 20x20x80mm was moulded by hot-pressing (at 180 $^{\circ}\text{C}$) mixture of CNSW and liquefied wood in accordance of weight ratio of 1:0.6 (Fig. 2(c)). CNSW, liquefied wood, and green body of WCs have been fired at 900 $^{\circ}\text{C}$ for 60 minutes in the CO_2 atmosphere.

The phase structure of the prepared samples was investigated using a Bruker D8 Advance diffractometer with $\text{Cu K}\alpha$ radiation ($\lambda = 0.154 \text{ nm}$). The experimental diffraction patterns were collected at room temperature by step scanning in the range of $5^{\circ} \leq 2\theta \leq 70^{\circ}$. The functional groups of woodceramics were determined by FTIR. The samples were milled, mixed with KBr powder and compressed to form a pellet. Spectra were recorded in air by using a Nicolet 6700 model. The morphological features of the prepared samples were examined using a field emission SEM (Hitachi S-4800 FE-SEM System, Japan) operated at an accelerating voltage of 10 kV. The Raman scattering spectra were recorded at room temperature using a Horiba Xplora Plus micro-Raman spectrometer. The measurements were performed with a laser excitation of 532 nm.

Table 1. The chemical composition of CNSW (%wt.).

C	N	O	H	Others
53.6	9.5	27.3	8.8	0.8

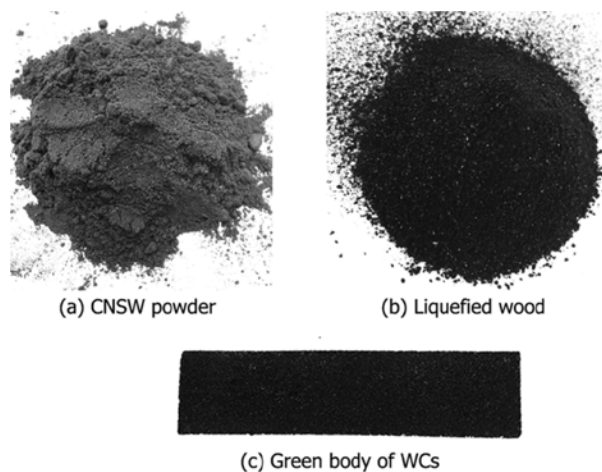


Fig. 2. (a) CNSW powder, (b) Liquefied wood, and (c) green body of WCs.

Results and discussion

Fig. 3 shows the XRD spectra of CNSW, liquefied wood, and WCs. The XRD spectra of the three samples are similar to each other and are typical ones of amorphous carbon which is fired at low temperatures. On each spectrum, there are two characteristic peaks. The first occurred at the diffraction angle $2\theta \approx 22.5^{\circ}$ corresponding to the planes with Miller indices (002). This peak corresponding to the Miller indices (002) represents a distance between planes of the hexagonal carbon structure [14]. And the second occurred at the diffraction angle $2\theta \approx 43^{\circ}$ corresponding to the planes with Miller indices (101). These two are the characteristic diffraction peaks of graphite carbon [15]. These peaks are unclear and the large peak width indicates that the graphite carbon structure of samples is not complete and exists as a turbostratic carbon [9].

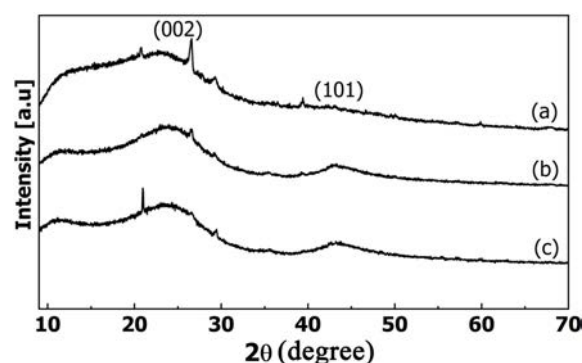


Fig. 3. XRD spectra of the samples fired at 900 $^{\circ}\text{C}$: (a)-Liquefied wood, (b)-CNSW, (c)-WCs.

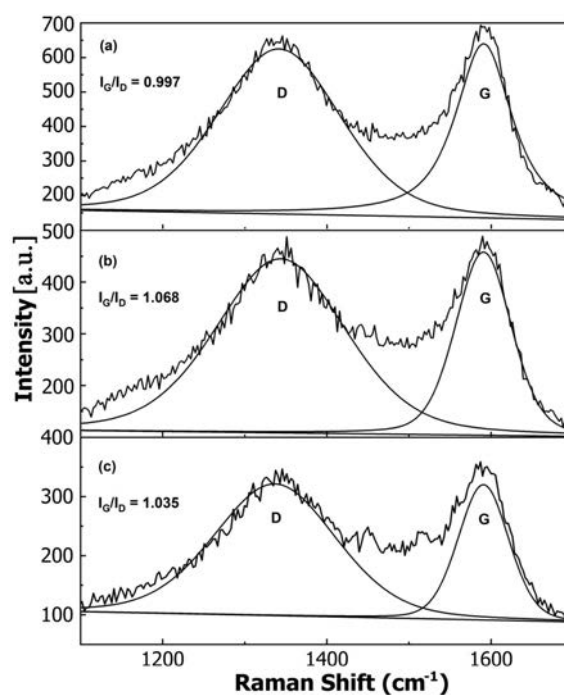


Fig. 4. Raman spectra of the samples fired at 900 $^{\circ}\text{C}$: (a)-Liquefied wood, (b)-CNSW, (c)-WCs.

Analysis of Raman spectra is a powerful method for evaluating graphite fraction in carbon materials. Results of the samples fired at 900 °C are shown in Fig. 4. The intensity and area of the amorphous carbon region correspond to the Raman shift at 1360 cm^{-1} (denoted by the letter D). The intensity and area of the graphite carbon region correspond to the Raman shift at 1590 cm^{-1} (denoted by the letter G). The Raman shift 1360 cm^{-1} characterizes the π -link of the C-C bond in the graphite crystal. The Raman shift 1590 cm^{-1} characterizes the σ -link in the C=C bond of the aromatic rings of the graphite crystal [16]. In Fig. 4, the Raman spectral regions of amorphous carbon (D) and graphite carbon (G) are overlapped each other, indicating an existence of turbostratic structure of carbon [17].

The graphitization degree can also be assessed by comparing the intensity ratio I_G/I_D of sample being accessed: the higher ratio I_G/I_D the higher graphitization degree the sample reached. The results showed that the ratio I_G/I_D of liquefied wood was 0.997, the ratio I_G/I_D of CNSW was 1.068 and I_G/I_D of WC was 1.035.

Liquefied wood is a disordered form, hard to graphitize. This is a feature of hard carbon. CNSW powder is more orderly structure than that of liquefied wood. Layers in the structure of graphite have been formed. The degree of graphitization of CNSW is higher than that of liquefied wood. This is also a feature of soft carbon. WCs is a composite of soft carbon and hard carbon. Soft carbon is formed from pyrolysis of CNSW powder, and hard carbon is formed from pyrolysis of liquefied wood. The degree of graphitization of WCs is an intermediate extent ($0.997 < 1.035 < 1.068$).

Chemical changes in the samples were investigated by using FTIR. Fig. 5 shows FTIR spectra of the samples before and after being heated at 900 °C in the CO_2 atmosphere. In Fig. 5, the curve 5b is the FTIR spectrum of the CNSW sample before being heated and the 5d is the FTIR spectrum of CNSW after being heated. Comparing these FTIR spectra, the intensity of the peaks shows that C-H_n (2854 cm^{-1}) was reduced, C=C (1632 cm^{-1}), and C=O (1720 cm^{-1}) were disappeared. At the same time, on the FTIR spectrum of the sample after being heated, there are peaks characterized for bonds of O-H (3100-3600 cm^{-1}), C-H_n (2925 cm^{-1}), C-O-C (1060 cm^{-1}), benzene ring (1516 cm^{-1}), C-O (1279 cm^{-1} , 1232 cm^{-1}), O-H (1232 cm^{-1}) (Table 2). The results in Table 2 and Fig. 6 indicate the change process of CNSW powder corresponding to the heating process. The covalent bonds of the functional groups were broken by the effect of temperature. The gases such as CO_x , NO_x , O_2 , H_2 , and N_2 were formed and evaporated in the heating process, the remaining solid was soft carbon.

The curve 5a (Fig. 5) is the FTIR spectrum of the liquefied wood before being heated and the curve 5c is the FTIR spectrum of the liquefied wood after

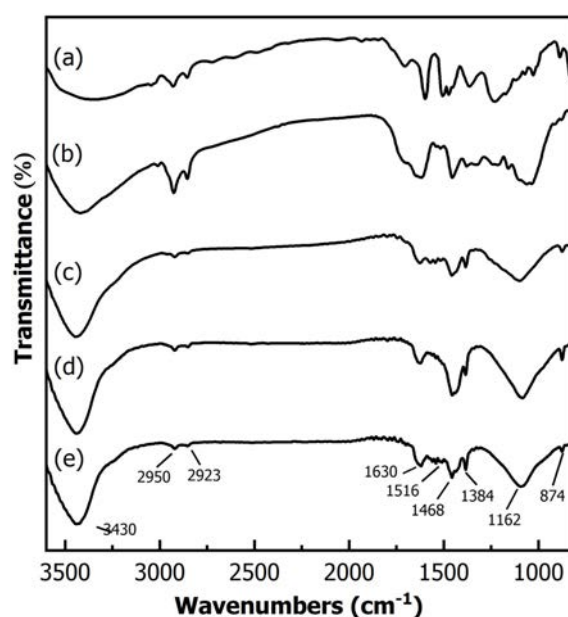


Fig. 5. FTIR spectra of the samples fired at 900 °C: (a), (b) liquefied wood and CNSW before being heated; (c), (d), (e) - liquefied wood, CNSW and WCs after being heated, respectively.

Table 2. The wavenumber of a functional group of soft carbon.

Wavenumber (cm^{-1})	Functional group	Ref.
3100-3600	O-H	[18, 19]
2925-2853	C-H _n	[18-20]
1720	C=O	[21]
1632	C=C	[20, 22]
1516	Benzene ring	[18,20]
1468	Aromatic CH ₂	[23]
1279	C-O	[20]
1232	C-O	[19]
1108	O-H	[18, 20, 22]
1060	C-O-C	[22]

Table 3. The wavenumber of a functional group of hard carbon.

Wavenumber (cm^{-1})	Functional group	Ref.
3100-3600	O-H	[18, 19]
2925-2853	C-H _n	[18-20]
1630-1628	Absorbed water	[21]
1516	Benzen ring stretch	[18, 20]
1468	Aromatic CH ₂	[23]
1384	Aromatic CH ₃	[23]
1275-1210	Ester	[21]
1162-1114	Phenol C-O	[21]
1075	benzyl hydroxyl C-O	[21]
881-874	Aromatic ring deformation	[21]

being heated. On the curve 5c there are new peaks corresponding to functional groups of the hard carbon. The hard carbon functional groups are represented in the Table 3.

In the heating process, liquefied wood was

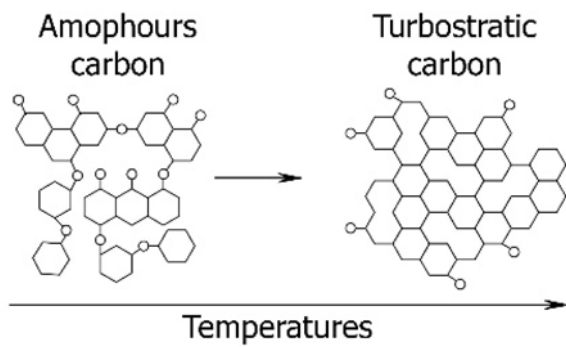


Fig. 6. The chemical change of CNSW powder.

decomposed; new chemical compounds such as phenol, toluence, o-methyl phenol, o-methylolphenol were converted through chemical reactions. They can be the chemical agents for reactions to form carbon fiber (Fig.

7) [24].

Fig. 8 shows the reaction that formed fiber carbon. The wavenumbers at 2923 cm^{-1} and 2853 cm^{-1} show the degradation of methylene bonds, indicating that the bonds were broken so that the benzene rings were formed carbon fibers (Fig. 5(a), 5(c)). This process is described by reaction (1) of o-methyl phenol to form 9, 10-dihydroanthracene that is a form of fiber carbon [23]. The wavenumbers at 3430 cm^{-1} of a hydroxyl group and at 1628 cm^{-1} of absorption water were decreased, indicating dehydration of hydroxyl group. The wavenumbers at 2922 cm^{-1} , 2854 cm^{-1} , and 1465 cm^{-1} correspond to the bonds of methylene. Further, the wavenumbers at 1602 cm^{-1} , 1508 cm^{-1} , and 1453 cm^{-1} corresponding to the bonds of $\text{C}=\text{C}$ of benzene ring were weakened. The wavenumbers

at $900\text{-}650\text{ cm}^{-1}$ corresponding to the bonds of C-H in the aromatic ring also were disappeared. Thus the

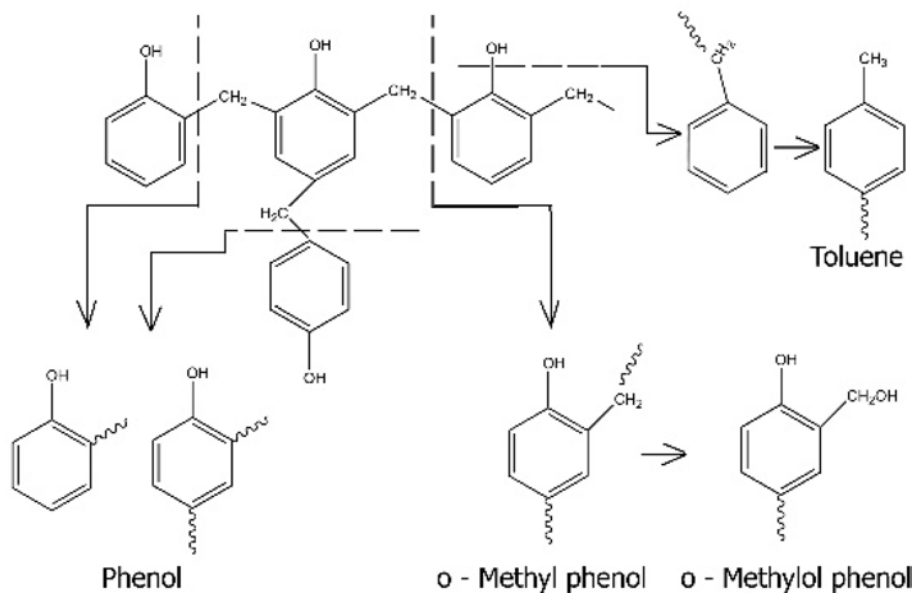


Fig. 7. The formula of products from the decomposition of liquefied wood.

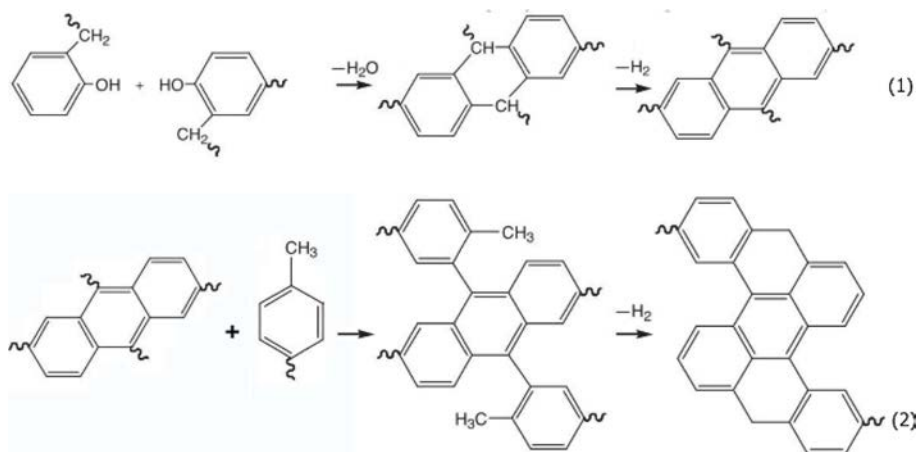


Fig. 8. The formula of formed fiber carbons.

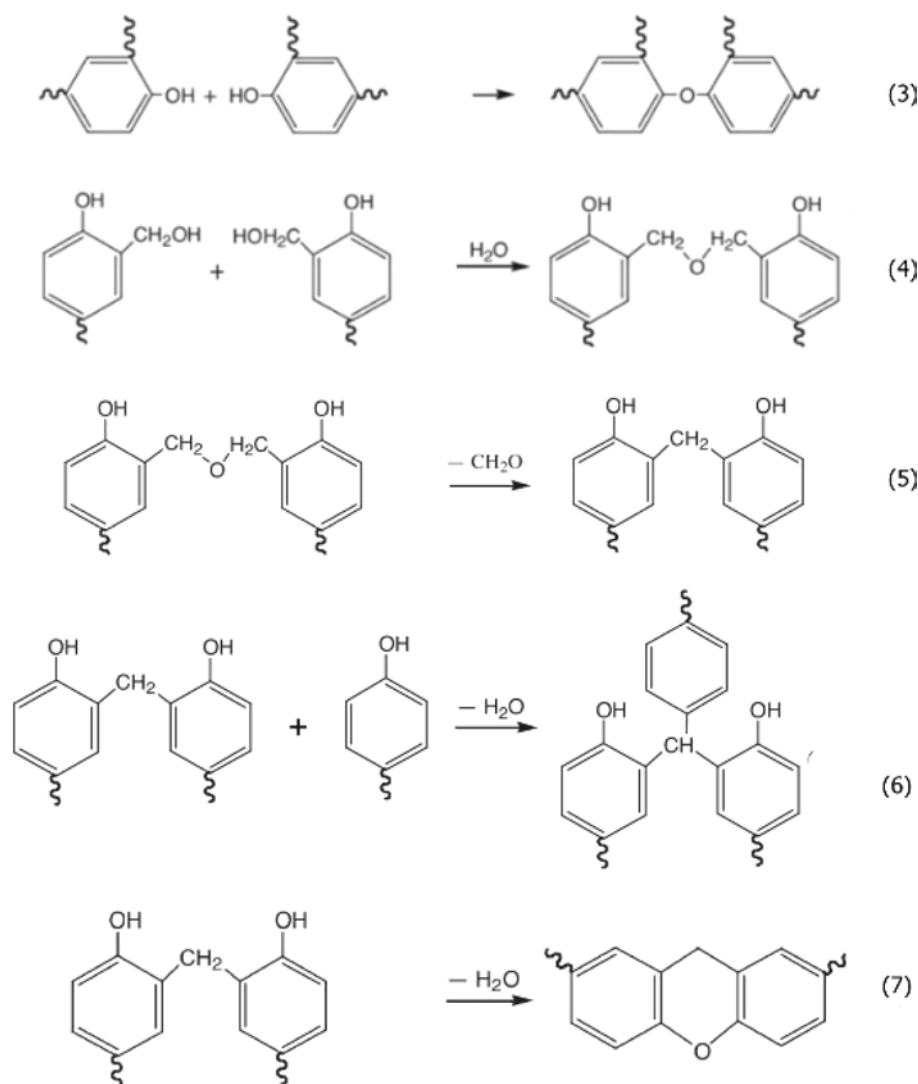


Fig. 9. The formation of byproducts during the sintering process.

benzene rings formed the carbon fiber. This process is described by the reaction (2) [23].

In addition to the above reactions, the thermal decomposition reaction of liquefied wood also formed by-products (Fig. 9). Wavenumbers at 1300-900 cm^{-1} correspond to the bonds of C-O, C-X or C-C. Wave numbers at 1220 cm^{-1} represents the ester linkage (-O-). Ester linkages were created by the condensation of phenolic hydroxyl and *o*-methylol phenol aromatic rings according to the reaction scheme (3), (4). The products of this reaction were 1,1'-oxydibenzene ester and 2,2'-(oxydimethenediyl) diphenol ester. On the FTIR spectrum of the product after being heated, there are the peaks at wavenumbers of 2923 cm^{-1} and 2853 cm^{-1} corresponding to methylene bridge (-CH₂-). The bridge of 2,2'-methanediyl diphenol was formed by the separation of formaldehyde (CH₂O) from 2,2'-(oxydimethenediyl) diphenol ether according to the reaction scheme (5). However, the intensity of the peak of the methylene bridges (at 2923 cm^{-1} and 2853 cm^{-1})

on the FTIR spectrum is weak, and the peak of the phenolic hydroxyl (at 1355 cm^{-1}) is unclear. That is to say, the hydroxymethyl groups were reacted with phenolic hydroxyl to form 2,2'-(phenylmethanediyl) diphenol (see the reaction scheme (6) or 2,2'-(phenylmethanediyl) decomposed water to form 9H-xanthene (reaction (7)). Compounds as 2,2'-(phenylmethanediyl) diphenol, 9H-xanthene and 1,1'-oxydibenzene ether are by-products of the heating process of liquefied wood [23].

The FTIR spectrum of WC (curve 5e) is a combination of the FTIR spectra of liquefied wood (curve 5c) and CNSW powder (curve 5d) after being heated. This confirms once again that WCs is a C/C composite of hard carbon and soft carbon.

Fig. 10 indicates SEM images of the samples after firing at 900 °C at magnification 300 times. Fig. 10(a) is a SEM image of the liquefied wood sample after being heated. It is a characteristic image of hard carbon [25]. We can see a SEM image of the sintered sample with many large pores. Because of an existence of high

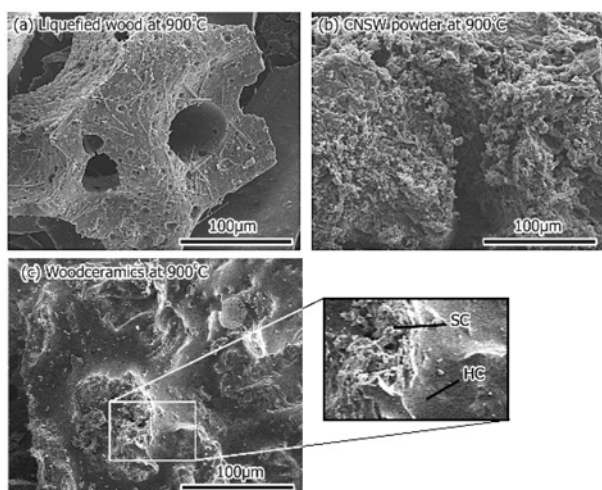


Fig. 10. The morphology of samples after heating at 900 °C, HC-hard carbon, SC-soft carbon.

amount of pores, the mechanical strength of the sintered liquefied wood sample was weak. The small fibers also can be seen in the SEM image. These are the carbon fibers as analyzed by FTIR method. Fig. 10(b) is a SEM image of the CNSW sample after being heated at 900 °C in the CO₂ atmosphere. We can see porous and discrete particles in the image. It is a characteristic of soft carbon after being heated [26]. Because of discrete particles, the sample does not have mechanical strength. Fig. 10(c) reveals a SEM image of the sintered WCs sample. Small pore scan be seen in this image. The mechanical strength of the WCs sample is higher than that of the liquefied wood sample. During the heating process, soft carbon was formed out of CNSW powder and hard carbon was formed out of the liquefied wood. The soft carbon filled into the pores of the hard carbon in order to form composite structure C (hard)/C (soft).

Conclusions

From the results of study (the chemical, the phase composition, the level of graphitization, the microstructure of the samples of CNSW, liquefied wood and WCs after being heated at 900 °C in the CO₂ atmosphere), we can conclude that the sintering process of the WC samples occurred during the chemical reactions. The products of decomposition reactions of the raw materials are different types of amorphous carbon named soft (turbostratic structure) and hard carbon. The hard carbon has a fiber structure. In the sintering process, soft carbon had filled up the pores in the sintered WCs material. The sintered WCs material can be considered as the composite material. In this composite, hard carbon is dispersing phase and soft carbon plays the role of base and/or bond phase.

Acknowledgments

To complete this research, the corresponding authors would like to thank the support from the doctoral scholarship program of Ho Chi Minh City University of Technology, Vietnam National University - Ho Chi Minh City. This research is partly funded by Vietnam National University Ho Chi Minh City (VNU-HCM) under grant number C2018-20-16.

References

- O. Ioannidou, and A. Zabaniotou, *Renew. Sust. Energ. Rev.* 11[9] (2000) 1966-2005.
- L.L. Zhang, and X.S. Zhao, *Chem. Soc. Rev.* 38[9] (2009) 2520-2531.
- W.E. Lee, and S. Zhang, *Int. Mater. Rev.* 44[3] (1999) 77-104.
- J. Cao, Q. Wang, and H. Dai, *Phys. Rev. Lett.* 90[15] (2003) 157601.
- A. Kumar, M. Gaim, D. Steininger, A.L. Yeyati, A. Martin-Rodero, A.K. Hüttel, and C. Strunk, *Phys. Rev. B: Condens. Matter* 89 (2014) 075428.
- A. Bianco, K. Kostarelos, and M. Prato, *Curr. Opin. Chem. Biol.* 9[6] (2005) 674-679.
- T. Okabe, K. Saito, and K. Hokkirigawa, *J. Porous Mater.* 2[3] (1995) 215-221.
- Y. Tao, P. Li, and S.Q. Shi, *Materials* 9[7] (2016) 540.
- H.M. Cheng, H. Endo, T. Okabe, K. Saito, and G.B. Zheng, *J. Porous Mater.* 6[3] (1999) 233-237.
- T. Okabe, K. Kakishita, H. Simizu, K. Ogawa, Y. Nishimoto, A. Takasaki, T. Suda, M. Fushitani, H. Togawa, M. Sata, and R. Yamamoto, *Trans. Mater. Res. Soc. Japan* 38[2] (2013) 191-194.
- J. Pan, X. Cheng, X. Yan, and C. Zhang, *J. Eur. Ceram. Soc.* 33[3] (2013) 575-581.
- D.L. Sun, X.C. Yu, D.B. Sun, and R. Wang, *Appl. Mech. Mater.* 190-191 (2012) 585-589.
- T. Hirose, B. Zhao, T. Okabe, and M. Yoshimura, *Mater. Sci.* 37[16] (2002) 3453-3458.
- A.K. Mishra and S. Ramaprabhu, *API Advances* 1[3] (2011) 032152.
- T. Hirose, T. Fujino, T. Fan, H. Endo, T. Okabe, and M. Yoshimura, *Carbon* 40[5] (2002) 761-765.
- L.B. Zhang, W. Li, J.H. Peng, N. Li, J.Z. Pu, S. M. Zhang, S.H. Guo, *Mater. Des.* 29[10] (2008) 2066-2071.
- M.L. Bauer, C.B. Saltonstall, Z.C. Leseman, T.E. Beechem, P.E. Hopkins, and P.M. Norris, *J. Heat Transfer* 138[6] (2016) 061302-061311.
- A. Nagaty, H. El-Sayed Osama, T.I. Samy, and Y.M. Olfat, *Holzforchung* 36[1] (1982) 29-35.
- V.P. Tolstoy, I. Chernyshova, and V.A. Skryshevsky, in "Handbook of Infrared Spectroscopy of Ultrathin Films" (Wiley Online Library, 2003).
- M. Aho, P. Kortelainen, J. Rantanen, and V. Linna, *J. Anal. Appl. Pyrolysis* 15 (1989) 297-306.
- Y. Huang, E. Ma, and G. Zhao, *Ind. Crop. Prod.* 69 (2015) 447-455.
- C. Morterra, and M.J.D. Low, *Mater.Lett.* 2[4] (1984) 289-293.
- H. Jiang, J. Wang, S. Wu, Z. Yuan, Z. Hu, R. Wu, Q. Liu, *Polym. Degrad. Stab.* 97[8] (2012) 1527-1533.
- K. Kirtania, J. Tanner, K.B. Kabir, S. Rajendran, and S.

- Bhattacharya, *Bioresour. Technol.* 151 (2014) 36-42.
25. R.S. Badu, and M. Pyo, *J. Electrochem. Soc.* 161[6] (2014) 1045-1050.
26. L. Ye, K. Wen, Z. Zhang, F. Yang, Y. Liang, W. Lv, Y. Lin, J. Gu, J.H. Dickerson, and W. He, *Adv. Energy Mater.* 6[7] (2016) 1502018.